International Journal of Nanomedicine

Dovepress

open access to scientific and medical research

Open Access Full Text Article

ORIGINAL RESEARCH

PLGA-*Astragalus* Polysaccharide Nanovaccines Exert Therapeutic Effect in Colorectal Cancer

Qian Cao[1,*], Ruijie Zhou[2,*], Songlin Guo[3], Kai Meng[4], Xiaojuan Yang[5], Miao Liu[1], Bin Ma[6], Chunxia Su[5], Xiangguo Duan[2]

[1]The First School of Clinical Medicine, Ningxia Medical University, Yinchuan, 750004, People's Republic of China; [2]School of Inspection, Ningxia Medical University, Yinchuan, 750004, People's Republic of China; [3]Institute of Medical Sciences, General Hospital of Ningxia Medical University, Yinchuan, Yinchuan, 750004, People's Republic of China; [4]Traditional Chinese Medicine Hospital of Ningxia Medical University, Yinchuan, 750003, People's Republic of China; [5]School of Basic Medical Sciences, Ningxia Medical University, Yinchuan, 750004, People's Republic of China; [6]Department of Oncology Surgery, the First People's Hospital of Yinchuan, Yinchuan, 750004, People's Republic of China

*These authors contributed equally to this work

Correspondence: Chunxia Su, School of Basic Medical Sciences, Ningxia Medical University, Yinchuan, 750004, People's Republic of China, Email 1651085195@qq.com; Xiangguo Duan, School of Inspection, Ningxia Medical University, Yinchuan, 750004, People's Republic of China, Email 2455281549@qq.com

Background: Tumor vaccines have achieved remarkable progress in treating patients with various tumors in clinical studies. Nevertheless, extensive research has also revealed that tumor vaccines are not up to expectations for the treatment of solid tumors due to their low immunogenicity. Therefore, there is an urgent need to design a tumor vaccine that can stimulate a broad anti-tumor immune response.

Methods: In this work, we developed a nanovaccine (NP-TCL@APS), which includes nanoparticles loaded with colorectal cancer tumor cell lysates (TCL) and Astragalus polysaccharides (APS) into poly (lactic-co-glycolic acid) to induce a robust innate immune response. The NP-TCL@APS was identified by transmission electron microscopy and Malvern laser particle size analyzer. The killing and immune activation effects of NP-TCL@APS were evaluated in vitro. Finally, safety and anti-tumor efficacy were evaluated in the colorectal cancer tumor-bearing mouse model.

Results: We found that NP-TCL@APS was preferentially uptaken by DC and further promoted the activation of DC in vitro. Additionally, nanoparticles codelivery of TCL and APS enhanced the antigen-specific $CD8^+$ T cell response and suppressed the growth of tumors in mouse models with good biocompatibility.

Conclusion: We successfully prepared a nanovaccine termed NP-TCL@APS, which can promote the maturation of DC and induce strong responses by T lymphocytes to exert anti-tumor effects. The strategy proposed here is promising for generating a tumor vaccine and can be extended to various types of cancers.

Keywords: colorectal cancer, nanovaccine, PLGA, *Astragalus* polysaccharide, tumor cell lysates (TCL)

Introduction

Colorectal cancer (CRC) is one of the most common types of malignant tumors, and has become a major threat to human life. The traditional treatment of malignant tumors is based on surgery, radiotherapy, and chemotherapy. However, many drawbacks induced by these traditional treatments remain challenge including immunosuppression, multiple organic toxicities as well as the risk of tumor recurrence.[1] Therefore, it is urgent to develop supplementary anti-tumor strategy with better therapeutic effectiveness and less toxicity in the treatment of cancer.

Currently, tumor vaccines are considered a promising method for treating tumors. However, the low immunogenicity limits their application. The whole tumor cell lysate (TCL) vaccine includes the entire sequence of mutated tumor antigens is concerned, which significantly improved immune response. It can activate polyclonal tumor-specific $CD8^+$ and $CD4^+$ T cells, thereby reducing the chance of immune escape.[2]

Received: 18 July 2024
Accepted: 1 September 2024
Published: 12 September 2024

Poly (lactic-co-glycolic acid) (PLGA) is a biodegradable polymer organic compound, with good biocompatibility, non-toxicity, and satisfactory microparticle- or nanoparticle-forming performance.[3] Studies have found that, in addition to acting as a drug delivery carrier, PLGA exerts a certain immune adjuvant effect; hence, it is also considered a particle adjuvant.[4] This polymer has been widely used for the preparation of particles as delivery systems of several therapeutic molecules, including vaccines. These PLA vaccine carriers have shown to induce a sustained and targeted release of different bacterial, viral and tumor-associated antigens and adjuvants, triggering distinct immune responses.[5]

Increasing evidences have demonstrated that polysaccharides from natural resources may provide promising strategy in the prevention or treatment of cancer.[6] *Astragalus* polysaccharides (APS), a main chemical component of *Astragalus*, enhance the immune function, and provide anti-viral, anti-bacterial, anti-tumor, anti-oxidant, and cardiovascular protection.[6] Acting as an immune adjuvant, APS plays an important anti-tumor role by promoting the maturation of dendritic cells (DC), thus activating cytotoxic T lymphocytes (CTL). Astragalus polysaccharide has a good ability to enhance antigenic immune response, and it was encapsulated in biocompatible materials PLGA as an immunostimulatory factor to form the delivery system.[7]

In this study, we developed a nanovaccine platform for CRC, which was prepared by simultaneously loading colon cancer TCL and APS into PLGA nanoparticles. Subsequently, a series of experiments were conducted to investigate the anti-CRC effect and mechanism of the nanovaccine, with the aim to provide new strategies and methods for the treatment of CRC.

Materials and Methods

Materials

PLGA was purchased from Shandong Academy of Medical Sciences (Taian, China). APS was purchased from Shanghai Yuanye Biotechnology Co., Ltd. (Shanghai, China). Poly (vinyl alcohol) (PVA) and carboxyfluorescein succinimidyl ester (CFSE) kits were purchased from Sigma–Aldrich. All antibodies used in flow cytometry were purchased from BD Biosciences (City, State, USA). MC38 cell line was purchased from Shanghai Yubo Biotechnology Co., Ltd. (Shanghai, China). DC 2.4 cell line was purchased from Shanghai Gaining Technology Co., Ltd. (Shanghai, China). MC38 and DC 2.4 cells were cultured in Dulbecco's modified Eagle's medium and RPMI-1640 medium, respectively. All cell culture media were supplemented with 10% fetal bovine serum (BI) and 1% antibiotics (penicillin and streptomycin; Beijing Solarbio Science and Technology Co., Ltd., Beijing, China). The two cell lines were incubated in a humidified environment at 37°C with 5% CO_2.

C57BL/6 mice (female, aged 6–8 weeks) were purchased from the Laboratory Animal Center of Ningxia Medical University (Yinchuan, China), and maintained in the same laboratory under specific pathogen-free conditions. All procedures for animal experiments were performed in line with the operating regulations of the Laboratory Animal Center of Ningxia Medical University and approved by the Animal Ethics Committee of Ningxia Medical University.

Preparation of TCL

MC38 cells were cultured in T75 flasks until they reached 80% confluency. The cells were detached with 0.25% trypsin and washed thrice with 1× phosphate-buffered saline (PBS). Next, the cells were freeze-thawed four times (ie, placement in liquid nitrogen for 10 min and at 37°C for 10 min). Subsequently, they were placed on ice and sonicated for 5 min (150 W, sonication for 3 s, interval for 3 s), and centrifuged for 30 min at 12,000 $r \cdot min^{-1}$. The supernatant (TCL) was collected, and the TCL concentration was determined by a bicinchoninic acid (BCA) protein quantitative kit. The pH of the TCL solution was adjusted to 8.5 using sodium bicarbonate. Fluorescein isothiocyanate (FITC) fluorescent dye was dissolved with dimethyl sulfoxide and prepared into a 10 mM reserve solution, shaken well, and stored in a −80°C deep freezer. Thereafter, freshly prepared FITC solution (50 μL) was slowly added to 1 mL of TCL solution, gently shaken, and kept in the dark for 8 h at room temperature.

Preparation of NP-TCL@APS

PLGA (100 mg) was dissolved in 2.4 mL of dichloromethane, and 200μL of TCL and 100μL of APS (10 mg·mL^{-1}) were added. The solution was placed on ice and subjected to sonication for 1 min (75 W, sonication for 3 s, interval for 3 s) to form the colostrum. The colostrum was slowly dripped into 4 mL 4% PVA solution, and subjected to sonication for 5 min (75 W, sonication for 3 s, interval for 3 s) to form double emulsion. The compound emulsion was slowly added to 20 mL of 0.1% PVA solution to solidify the nanoparticles, and the dichloromethane was volatilized by magnetic stirring for 3 h. After centrifugation at 12,000 r for 5 minutes, the supernatant was collected to test the encapsulation rates of TCL and APS. Following ultra-pure water suspension centrifugal precipitation, centrifugation was repeated at 12,000 r for 5 minutes; this step was repeated thrice to wash the nanoparticles.

Characterization of NP-TCL@APS

The morphology of NP-TCL@APS was observed by transmission electron microscopy. The particle size, potential, polymer dispersity index (PDI), and storage stability of NP-TCL@APS were determined using a Malvern laser particle size analyzer (Britain). Briefly, NP-TCL@APS was dissolved in ultra-pure water and stored at 4°C. NP-TCL@APS particle size, potential, and PDI were measured on days 1, 7, 14, and 21. The encapsulation of APS was evaluated by the phenol-sulfuric acid method. The encapsulation of TCL was examined by BCA protein quantification. Briefly, the concentration of APS and TCL in the supernatant was measured after centrifugation. The following formula was used to calculate the encapsulation rate:

$$\text{Encapsulation rate} = (\mathrm{W_{total}} - \mathrm{W_{free}})/\mathrm{W_{total}} \times 100\%,$$

where W_{total} and W_{free} indicate drug input and free drug, respectively.

The release of APS was measured with the phenol-sulfuric acid method. Briefly, 1 mg NP-TCL@APS was dissolved in 1 mL PBS and placed in a shaker at 37°C for 200 r·min^{-1} shock. After 24 h, the solution was centrifuged and the supernatant was obtained; this process was repeated for 7 days. The release of TCL was observed by sodium dodecyl sulfate-polyacrylamide gel electrophoresis (SDS-PAGE). The cumulative release of TCL and APS was measured by the BCA and phenol-sulfuric acid methods.

Measurement of the Cytotoxicity of NP-TCL@APS

The toxicity of NP-TCL@APS to DC was investigated using the Cell Counting Kit-8 (CCK8; SEVEN Innovation, Beijing, China). Briefly, DC 2.4 cells were seeded into a 96-well plate (1×10^4 /well), and the concentration gradient of NP-TCL@APS was set as follows: 500, 250, 125, 62.5, 31.25, 15.62, 7.81, 3.91, 1.95, 0 mg·mL^{-1}. At 24 h after vaccine intervention in DC 2.4 cells, the CCK8 reagent was added; 4 h later, the absorbance was measured at 450 nm wavelength. Cell viability was calculated using the following formula:

$$\text{Cell viability}\,(\%) = (\mathrm{A_{dosed}} - \mathrm{A_{blank}})/(\mathrm{A_{no\ dosed}} - \mathrm{A_{blank}}) \times 100\%,$$

where A_{dosed} denotes the absorbance of cells, drugs, and CCK8; A_{blank} denotes the absorbance of medium and CCK8; and $A_{no\ dosed}$ denotes the absorbance of cells and CCK8.

Measurement of NP-TCL@APS Uptake by DC 2.4 Cells

Firstly, the uptake of NP-TCL@APS by DC 2.4 cells was observed through fluorescence microscopy. Briefly, a circular slide was placed in a 24-well plate, and 1×10^5 DC 2.4 cells were added. Following cell adhesion, FITC-labeled NP-TCL @APS was added. After 24 h, the culture medium was discarded, and the cells were washed thrice with PBS. Next, cell membrane dye 1.1'-dioctadecyl-3,3,3',3'-tetramethylindocarbocyanine perchlorate (DiI) at a concentration of 10 mM was added. Following incubation at 37°C for 30 min, the supernatant was discarded and the cells were washed thrice with PBS. Thereafter, the cells were fixed in 4% paraformaldehyde for 10 min and washed thrice with PBS. Droped the 4',6-diamidino-2-phenylindole (DAPI) sealer on the slide, gently clipped the slide with tweezers, adhesion cells face down, covered on the sealer. The uptake of NP-TCL@APS by DC 2.4 cells was observed using a fluorescence microscope (Nikon, TOKYO, JAPAN).

Secondly, the efficiency of NP-TCL@APS uptake by DC 2.4 cells was measured by flow cytometry. Briefly, 1×10^5 cells were seeded into a 12-well plate. Following cell adhesion, FITC-labeled NP-TCL@APS was added. After 24 h, the cells were collected, washed once with PBS, and measured by flow cytometry (FACSCelesta TM, BD).

Measurement of the Effect of NP-TCL@APS on Maturation

The expression levels of major histocompatibility complex class II (MHCII), CD86, and CD80 on DC 2.4 cells were measured by flow cytometry. Briefly, 1×10^5 cells were seeded into a 12-well plate. Following cell adhesion, NP-TCL @APS was added. After 24 h, the cells were collected and resuspended in 100μL of PBS, cells were stained with antibodies (0.5μL) against surface markers (MHCII, CD86, and CD80, and the cells were placed at 4°C for 30 min. Subsequently, the supernatant was removed by centrifugation, and the cells were resuspended in PBS. Stained cells were finally evaluated by flow cytometry. The levels of cytokines interleukin-6 (IL-6) and IL-12p40 secreted by DC were measured using the enzyme-linked immunosorbent assay (ELISA) kit (BD Biosciences).

Lymphocytes Activated by NP-TCL@APS Exert Anti-Tumor Effects in vitro

Activated DC were co-cultured with splenic lymphocytes at a ratio of 20:1 for 48 h. Lymphocyte proliferation was measured by CCK8 and carboxyfluorescein succinimidyl ester (CFSE). Activated DC were co-cultured with splenic lymphocytes from mouse at a ratio of 20:1 for 48h.Then collected the cells and added the surface antibodies and incubated at 4°C for 30 in the dark, after the permeabilization solution treatment, performed the intracellular staining, cells were stained with antibodies (granzyme B, perforin, tumor necrosis factor-α and interferon-γ). The levels of granzyme B (GZMB), perforin, tumor necrosis factor-α (TNF-α), and interferon-γ (IFN-γ) secreted by $CD8^+$ T cells were measured by flow cytometry. Activated lymphocytes were co-cultured with MC38 cells at 10:1 for 48 h. MC38 cell proliferation was measured by CCK8 and CFSE.

Evaluation of the Safety and Anti-Tumor Effect of NP-TCL@APS in vivo

MC38 cells were subcutaneously injected into the right flank of mice on day 1. NP-TCL@APS (100μL) was subcutaneously administered in the groin area of mice on days 5, 14, and 21. The weight of mice and tumor size were recorded every 48 h, and the growth curve and tumor change curve were drawn. On day 28, the mice were sacrificed; the tumors were removed and photographed, and their weight and volume were measured. The formula used to calculate the volume was as follows:

$$\text{Tumor volume}\left(\text{mm}^3\right)=\left(\text{long diameter}\times\text{short diameter}^2\right)/2$$

Pathological changes in the heart, liver, and kidneys of mice were measured by hematoxylin-and-eosin staining.

Mechanism Underlying the Anti-Tumor Effect of NP-TCL@APS

Single-cell suspension was obtained from the spleen, tumor, and inguinal lymph nodes of mice. Flow cytometry was used to detect the infiltration of $CD8^+$ and $CD4^+$ T cells in the tumor, the expression levels of negative immune regulatory molecules PD-1 and T cell Immunoglobulin and ITIM Domain (TIGIT), and the number of M1 macrophages. The levels of MHCI, MHCII, and CD80 expressed by DC in the spleen and lymph nodes of mice, the number of $CD8^+$ T cells and their secretion levels of GZMB, TNF-α, and IFN-γ, the number of $CD4^+$ T cells and their secretion levels of TNF-α, IFN-γ, and IL-17 were detected by flow cytometry. The expression of PD-1 and TIGIT in $CD8^+$ and $CD4^+$ T cells was also investigated.

Statistical Analysis

The normality of data was tested using SPSS version 23.0 (IBM Corp., Armonk, NY, USA). For non-normally distributed data, two-tailed test, analysis of variance, and Student–Newman–Keuls-q test were used. For data not distributed by the median and interquartile spacing, a non-parametric test of two independent samples was used for comparison between two groups; a non-parametric test of k independent samples was used for comparison between multiple groups. Data are expressed as the mean ± standard deviation after the normality test. p-values <0.05 denote statistically significant differences.

Results

Preparation and Characterization of NP-TCL@APS

Firstly, PLGA nanoparticles loaded with TCL and APS were prepared by a two-emulsion solvent volatilization method (Figure 1A). Transmission electron microscopy images indicated that the well-dispersed nanoparticles had a spherical and uniform morphology (Figure 2A). The diameter of four nanoparticles, namely NP-Empty (containing ultra-pure water), NP-TCL (containing TCL), NP@APS (containing APS), and NP-TCL@APS (containing both TCL and APS), was detected (Figure 2B). The PDI of all nanoparticles was <0.2, indicating that the size distribution was homogeneous. All four nanoparticles were negatively charged; hence, they exhibited good dispersion in aqueous solutions and did not aggregate. The surface charge of NP-Empty and NP@APS was approximately −20 mV, while that of NP-TCL and NP-TCL@APS was approximately −10 mV. These results indicated that TCL packaging can increase the surface charge of nanoparticles (Table 1). The stability of the nanovaccine was assessed by monitoring changes in particle size stored at 4°C for different time periods. Moreover, it was found that all four nanoparticles maintained good dimensional stability (Figure 2C). The encapsulation efficiency of APS and TCL in NP-TCL@APS was 64.11±5.22% and 78.22±6.34%, respectively. SDS-PAGE was used to confirm the sustained release effect of NP-TCL@APS, as shown in (Figure 2D). By comparing the groups of bands, we observed that TCL release peaked in the first 3 days and was slowly reduced thereafter; APS also showed a comparable release profile (Figure 2E). According to these results, NP-TCL@APS may be used in in vitro and in vivo studies.

Evaluation of the Anti-Tumor Effect of NP-TCL@APS in vitro

We sought to assess the safety of the vaccine against normal immune cells. Thus, the CCK8 assay was used to measure the toxicity of NP-TCL@APS to DC. As shown in Figure 3A, NP-TCL@APS did not exert an obvious toxic effect on DC, further confirming the safety of the vaccine. Fluorescence microscopy was used to observe the uptake of NP-TCL @APS by DC 2.4 cells (Figure 3B). Compared with the control, green fluorescence was visible in both the TCL+APS and NP-TCL@APS groups. Importantly, the fluorescence signal of the NP-TCL@APS group was obviously stronger, suggesting better uptake by DC. Flow cytometry analysis to determine the uptake efficiency of NP-TCL@APS in DC 2.4 cells (Figure 3C) yielded consistent results.

Activation of DC is a prerequisite for NP-TCL@APS to exert its anti-tumor effects. To elucidate the effects of NP-TCL@APS on DC, DC 2.4 cells were treated and cultured in different groups for 48 h. Compared with other treatments, NP-TCL@APS promoted the expression of antigen-presenting cells (APC) functional molecules, including MHCII, CD86, and CD80 (Figure 3D). In addition, the levels of cytokines IL-6 and IL-12p40 secreted by DC were significantly increased after treatment with APS, NP-Empty, NP@APS, and NP-TCL@APS (Figure 3E). Moreover, DC pretreated with NP-TCL@APS exhibited higher antigen-presenting ability versus untreated DC, as revealed by the increased proliferation of T cells (Figure 3F and G) and cytokine secretion (Figure 3H) by lymphocytes. Next, we evaluated the cytotoxic effect of the vaccine on the CRC cell line MC38 in vitro. Compared with the other treatments, NP-TCL@APS

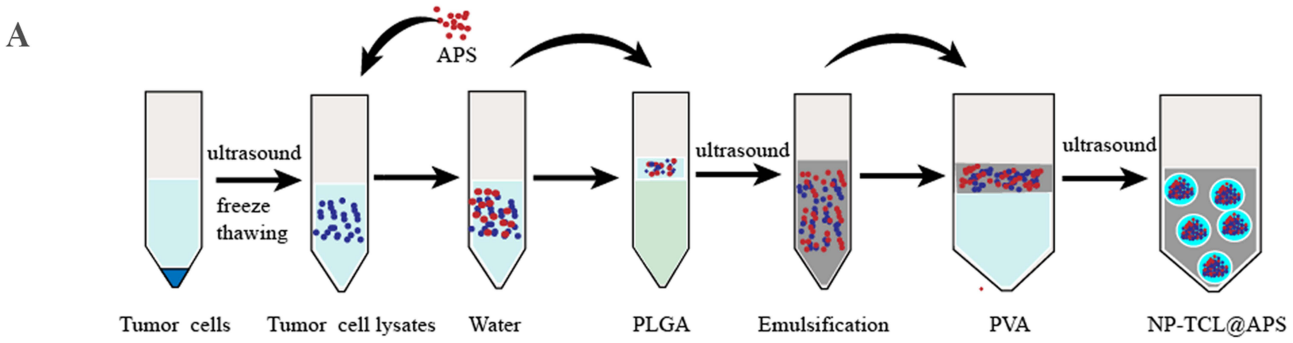

Figure 1 (**A**) Schematic depiction of NP-TCL@APS preparation.
Abbreviations: APS, *Astragalus* polysaccharides; NP, nanoparticles; TCL, tumor cell lysate.

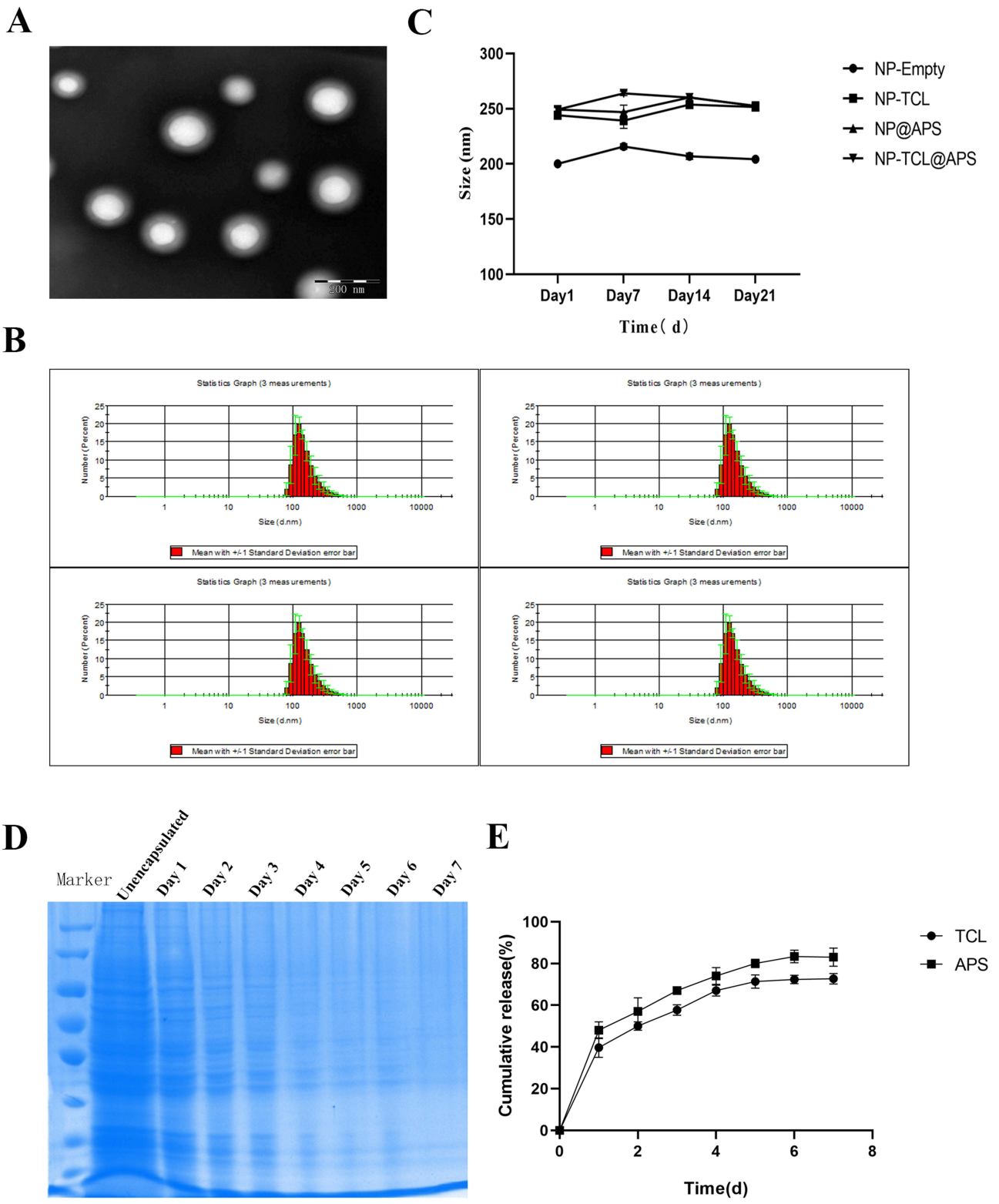

Figure 2 Characterization of NP-TCL@APS. (**A**) Transmission electron microscopy (TEM) was used to observe the micromorphology of NP-TCL@APS. (**B**) The laser particle size analyzer detected the particle size of NP-TCL@APS. (**C**) Storage stability of NP-TCL@APS. (**D**) SDS-PAGE detected the release of TCL in NP-TCL@APS. (**E**) Release curves of TCL and APS in NP-TCL@APS.

Table 1 Statistical Results of Nanoparticle Size, Potential, and PDI (x ± s, n=3)

Group	Particle size (nm±SD)	Potential (mV±SD)	PDI±SD
NP-Empty	200.07±2.6	−23.1±0.231	0.177±0.006
NP-TCL	244.1±2.1	−12.8±0.107	0.192±0.052
NP@ APS	249.3±2.2	−20.6.6±0.229	0.104±0.021
NP -TCL@ APS	249.17±1.54	−11.3±0.138	0.141±0.007

significantly inhibited the proliferation of MC38 cells (Figure 3I) and induced a stronger cytotoxic effect (Figure 3J). These results indicated that NP-TCL@APS has a good safety profile and antigen presentation function in vitro, which plays an important role in the process of T cell activation and further killing of tumor cells.

Inhibition of Tumor Growth by NP-TCL@APS in vivo

NP-TCL@APS exhibited high efficacy for inducing an effective immune response and tumor cell death in vitro. This finding prompted us to explore whether the activated immune response can inhibit tumor growth in tumor-bearing mice. The MC38 tumor model was established (Figure 4A). PBS control did not inhibit tumor growth. In contrast, NP-Empty, NP@APS, NP-TCL, and NP-TCL@APS suppressed tumor growth. Among them, NP-TCL @APS demonstrated the maximum therapeutic effect and, at the end of monitoring, the greatest reduction in tumor

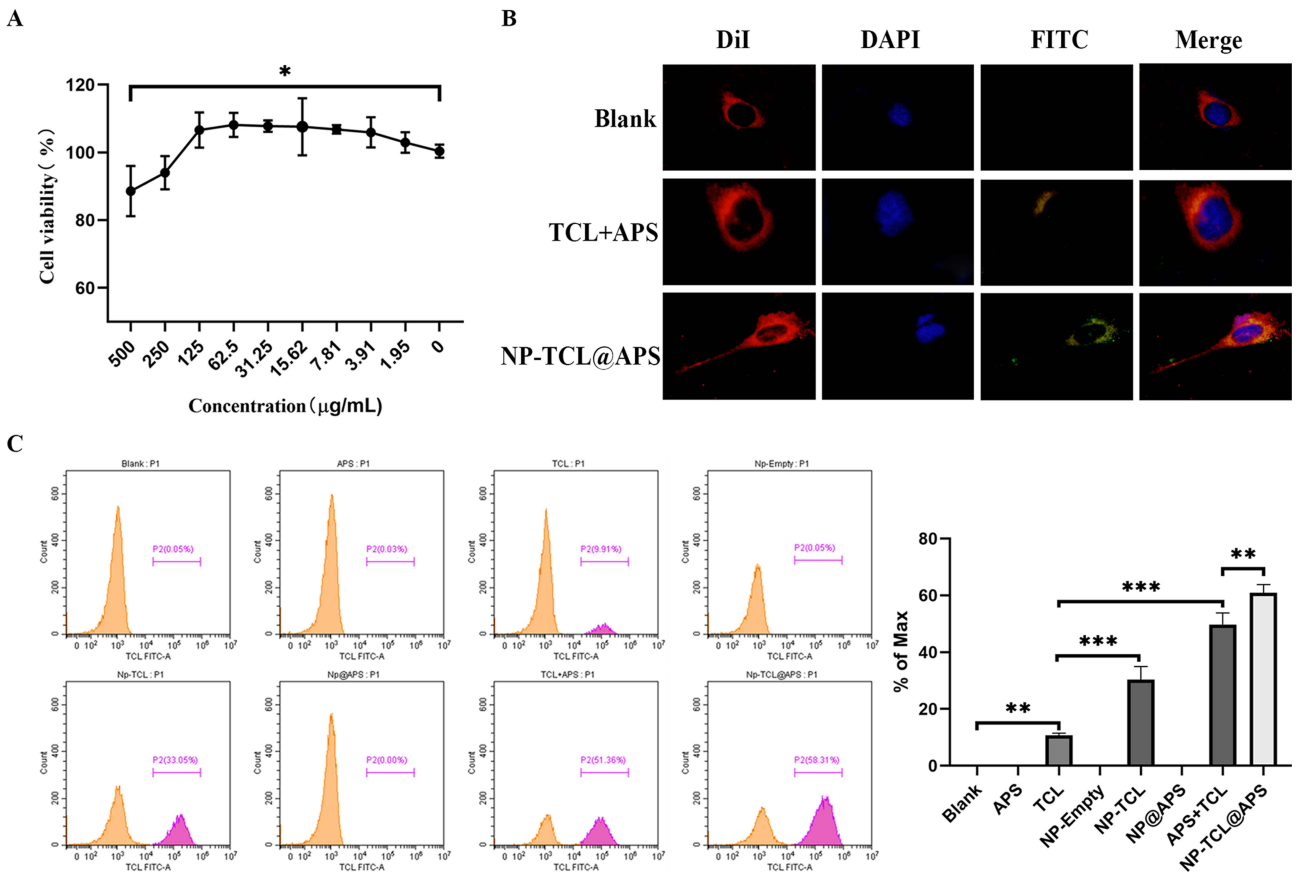

Figure 3 Continued.

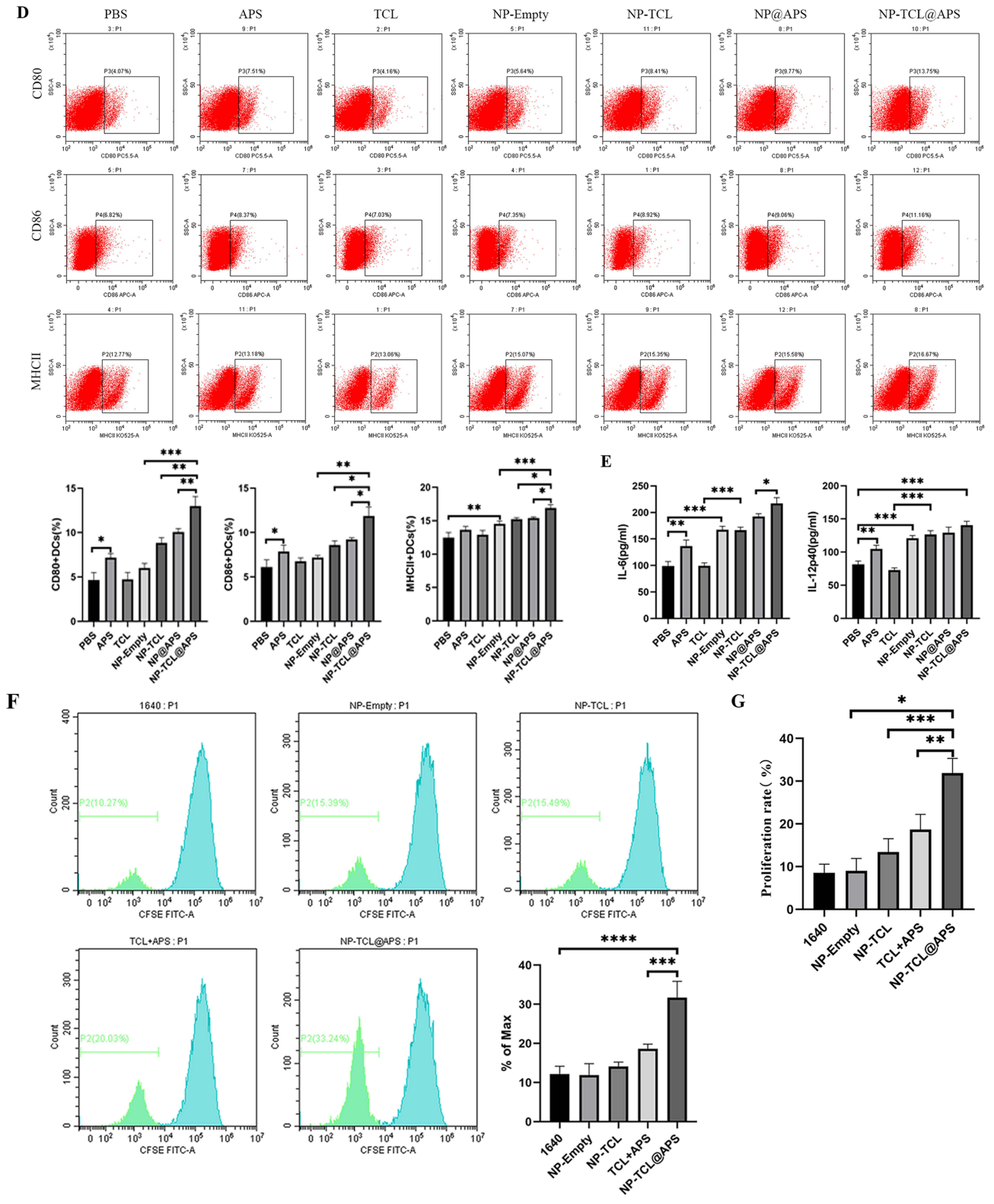

Figure 3 Continued.

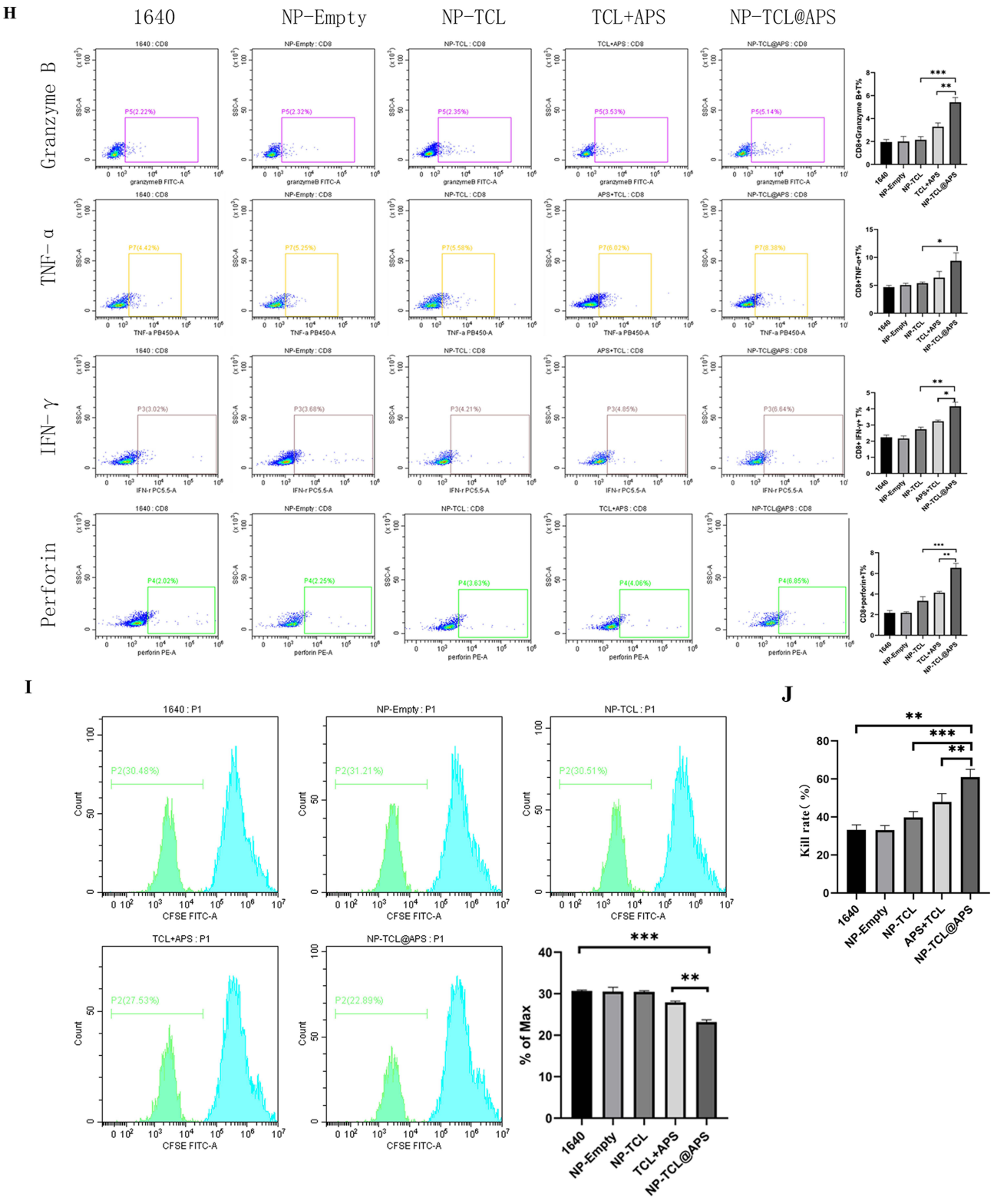

Figure 3 Evaluation of the anti-tumor effect of NP-TCL@APS in vitro. (**A**) The toxicity of NP-TCL@APS to BMDC was evaluated by CCK8. (**B**) Fluorescence microscopy detected the uptake of NP-TCL@APS by DC 2.4 cells. (**C**) FCM detected the efficiency of NP-TCL@APS uptake by DC 2.4 cells. (**D**) FCM detected the expression of MHCII molecules and co-stimulatory molecules CD80 and CD86 on the surface of BMDC. (**E**) ELISA detected the levels of cytokines IL-6 and IL-12p40 secreted by BMDC. (**F**) CFSE detected NP-TCL@APS-activated DC that promoted lymphocyte proliferation. (**G**) CCK8 detected NP-TCL@APS-activated DC that promoted lymphocyte proliferation. (**H**) FCM detected the effect of NP-TCL@APS-activated DC on the activation of $CD8^+$ T cells. (**I**) CFSE detected the effect of activated lymphocytes on the proliferation of MC38 cells. (**J**) CCK8 detected the cytotoxic effect of activated lymphocytes against MC38 tumor cells. *p <0.05, **p <0.01, ***p <0.001.

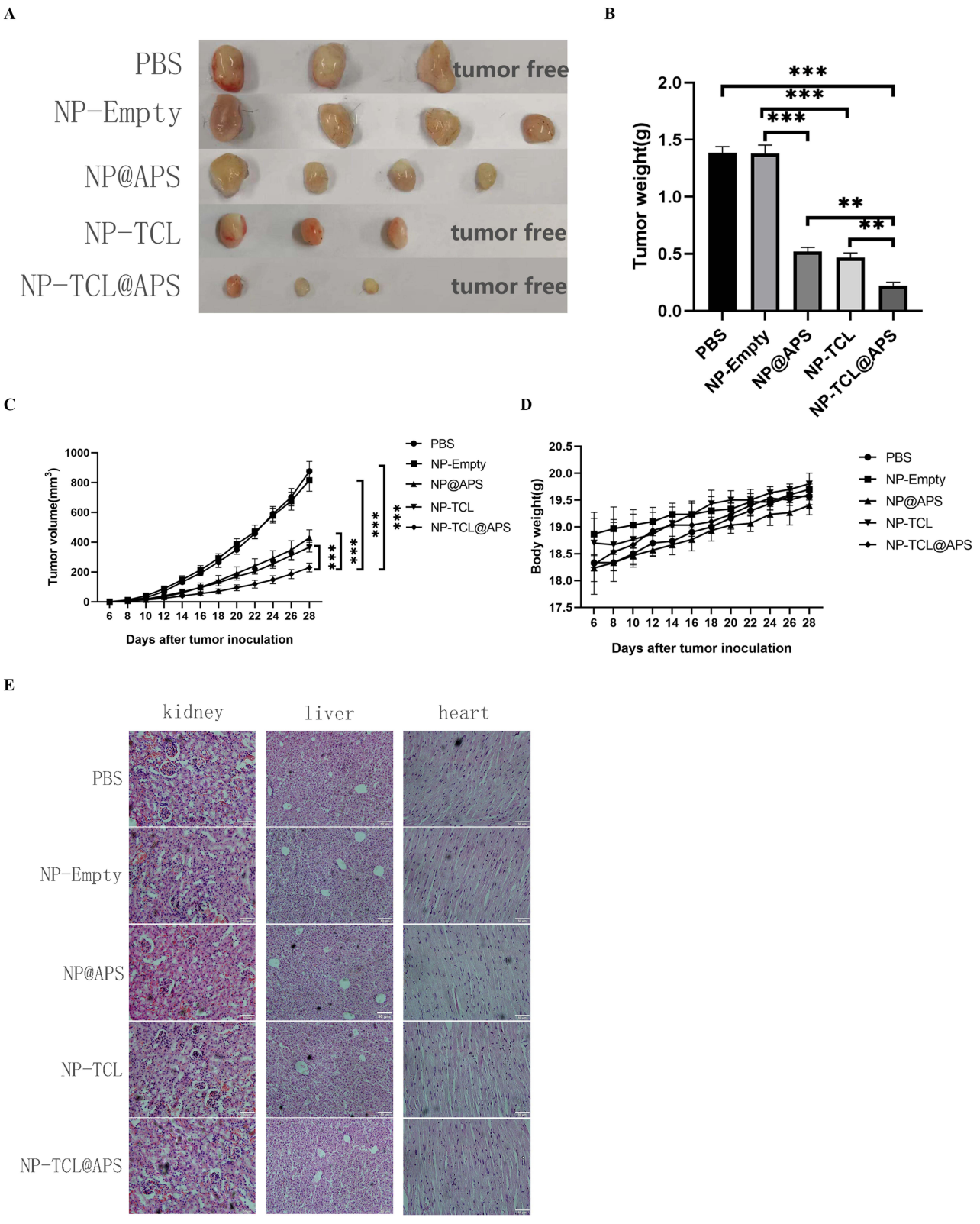

Figure 4 Evaluation of the anti-tumor effect and safety of NP-TCL@APS in vivo. (**A**) Tumor image. (**B**) Tumor weight. (**C**) Changes in mouse tumor volume. (**D**) Changes in mouse body weight. (**E**) Hematoxylin-and-eosin staining detected pathological changes in the heart, liver, and kidneys of mice. $^{**}p<0.01$, $^{***}p<0.001$.
Abbreviations: APS, *Astragalus* polysaccharides; NP, nanoparticles; TCL, tumor cell lysate.

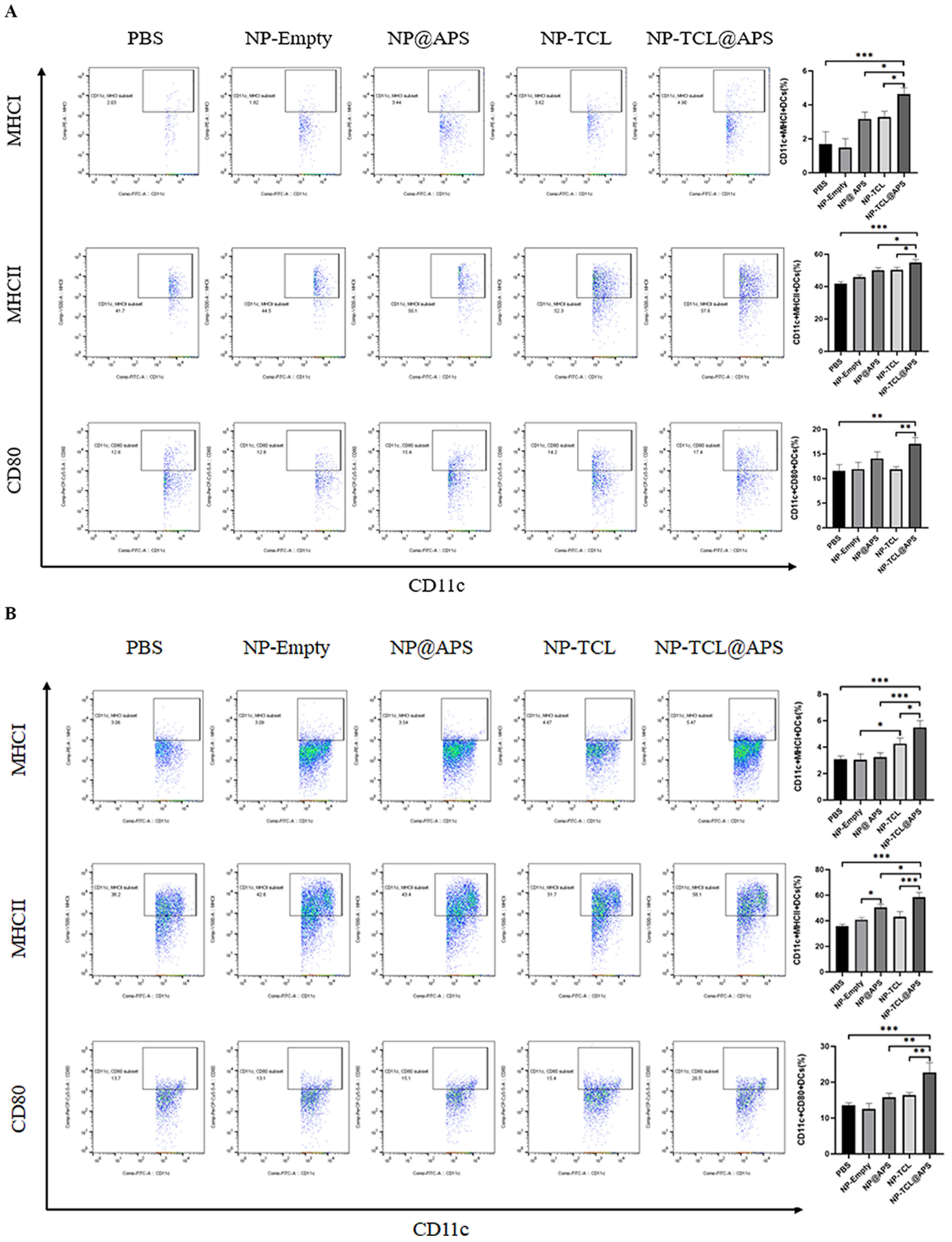

Figure 5 Continued.

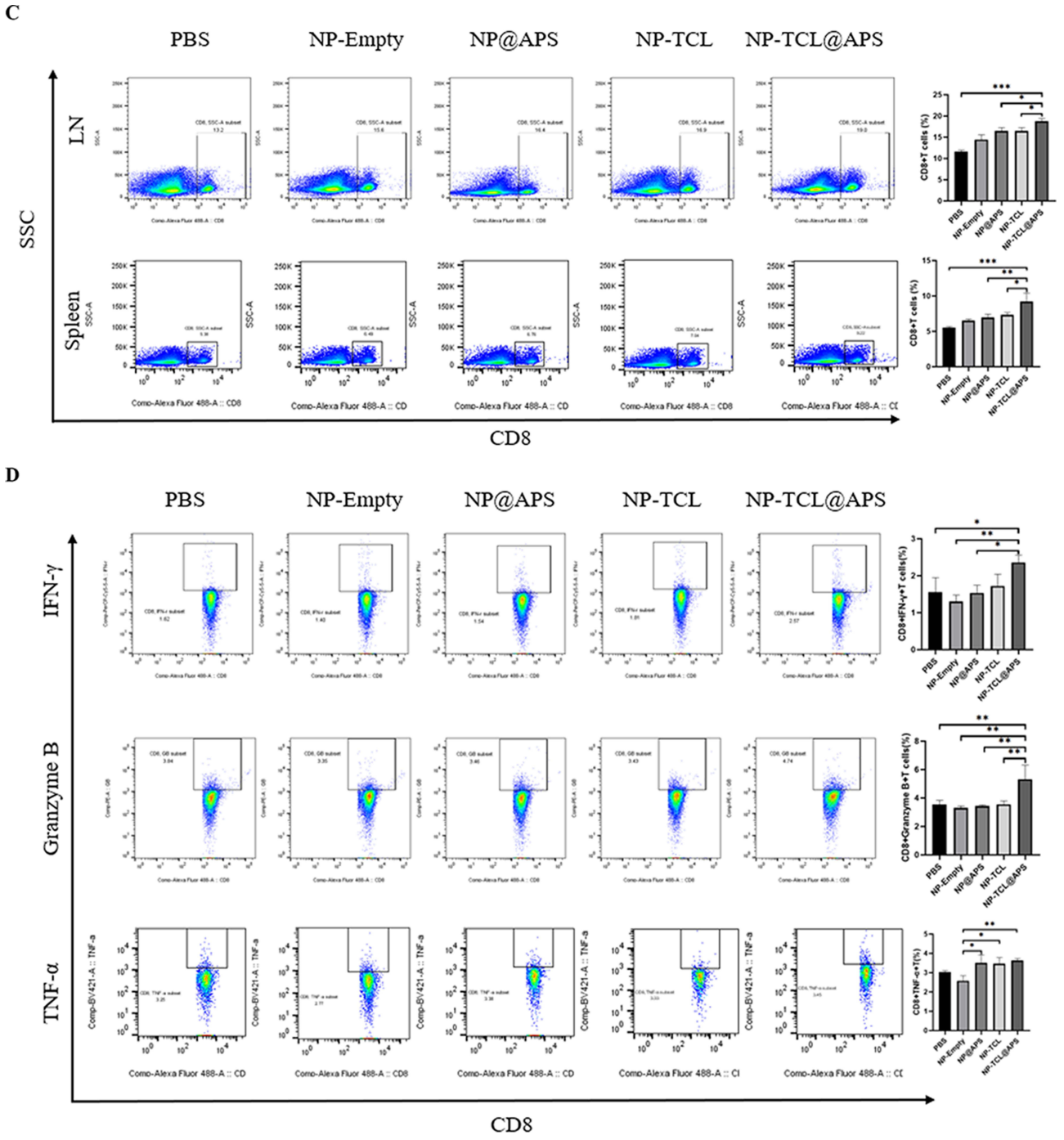

Figure 5 Continued.

weight and volume (Figure 4B and C). We also monitored the body weight of mice in the different groups. During the monitoring period, there were no differences observed in the body weight of mice (Figure 4D). In addition, the major organs of the mice were extracted for pathological morphological analysis. The results of hematoxylin-and-eosin staining showed that there were no obvious pathological morphological abnormalities in the main organs of the mice treated with NP-TCL@APS. These results indicate that NP-TCL@APS had good biocompatibility (Figure 4E).

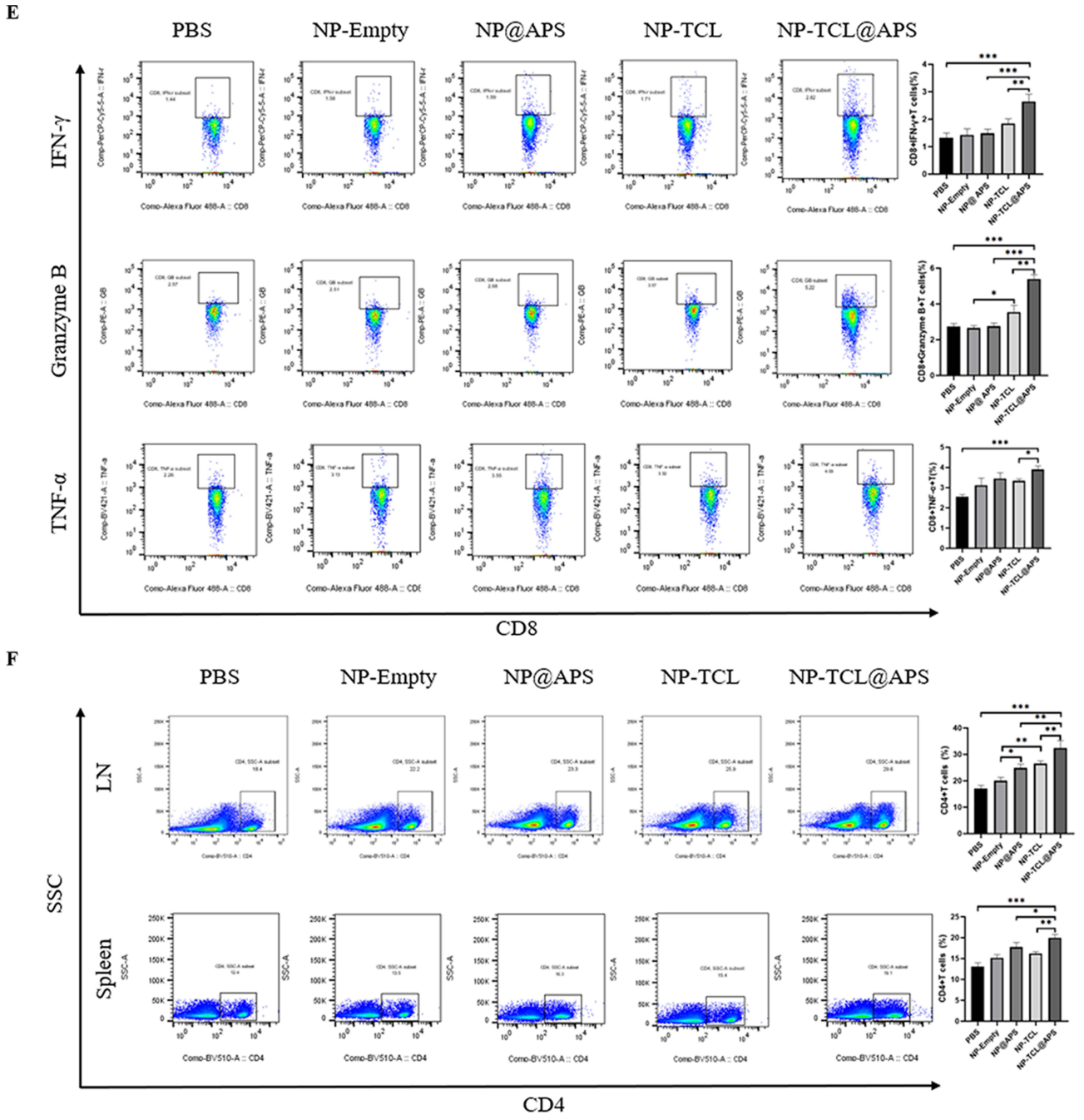

Figure 5 Continued.

NP-TCL@APS Played an Anti-Tumor Role by Activating the Immune System

As antigen-presenting cells, DC are the core participants of the immune system and important regulators of innate and acquired immune responses. Thus, they play a critical role in the immune response to tumors. To elucidate the effects of NP-TCL@APS on DC, we removed the spleen and inguinal lymph nodes of mice and measured the expression of MHCI, MHCII, and CD80 on $CD11c^+$ DC by flow cytometry. As expected, the expression of MHCI, MHCII, and CD80 was upregulated both in the spleen and lymph nodes after treatment with NP-TCL@APS (Figure 5A and B). These results indicate that NP-TCL @APS induced DC maturation more effectively compared with the other treatments.

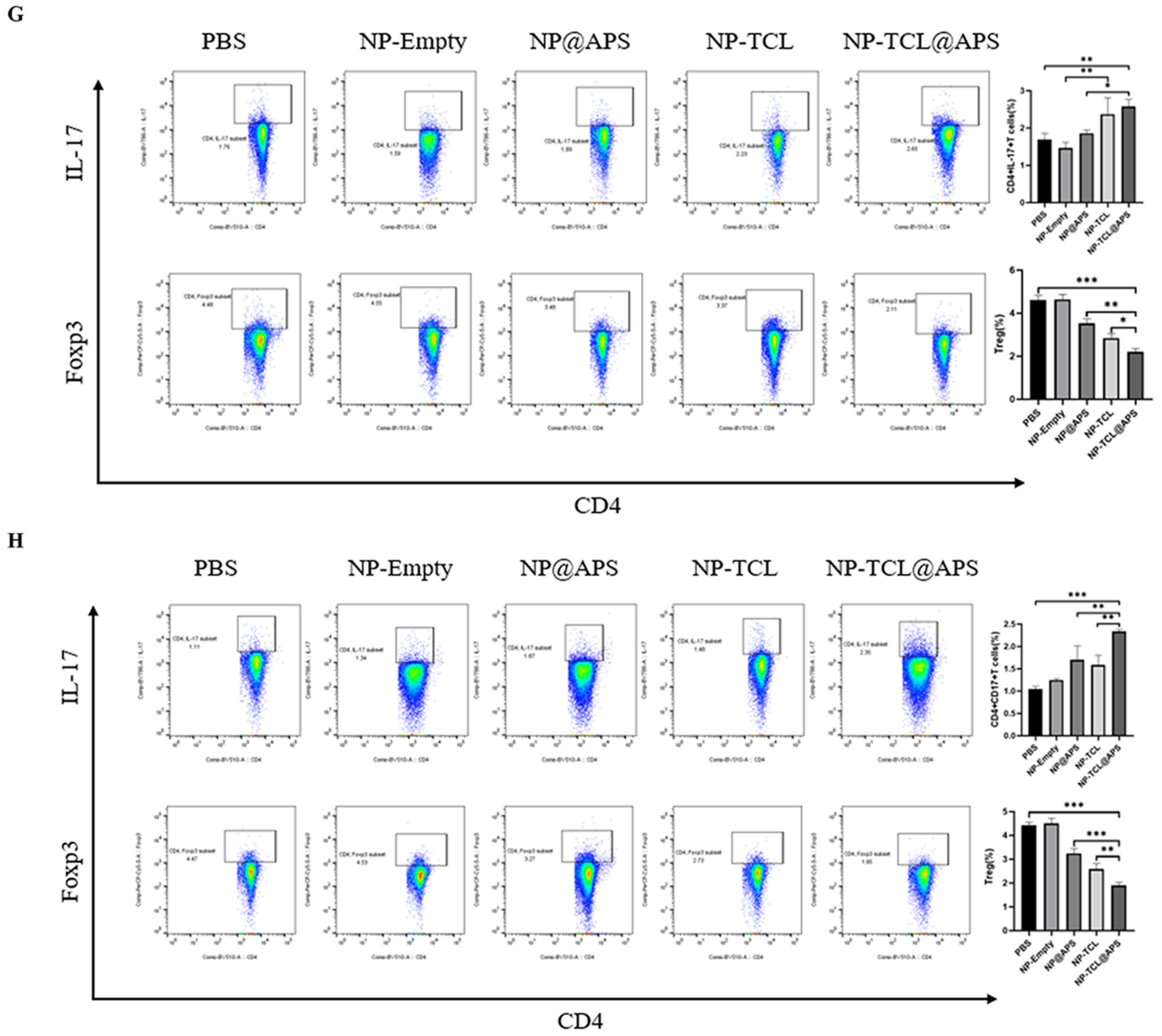

Figure 5 Continued.

Mature DC present tumor antigens to T cells and induce T cell activation. Therefore, we further analyzed the $CD8^+$ T cells and the levels of cytokines in the spleen and lymph nodes using flow cytometry. Notably, NP-TCL@APS induced the greatest number of $CD8^+$ T cells and higher expression of TNF-a, IFN-γ, and GZMB compared with the other treatments (Figure 5C–E). In addition, flow cytometry displayed that NP-TCL@APS increased the number of $CD4^+$ T cells in the spleen and lymph nodes compared with PBS, NP@APS, and NP-TCL (Figure 5F). Consistent with the aforementioned data, NP-TCL@APS could promote the secretion of IFN-γ and TNF-α by $CD4^+$ T cells compared with the other treatments (Figure 5I and J).

Moreover, compared with PBS, NP-TCL, and NP@APS, NP-TCL@APS decreased the number of regulatory T (Treg) cells and increased that of T helper 17 (Th17) cells in the spleen and lymph nodes (Figure 5G and H). Finally, we measured the number of $CD8^+$ and $CD4^+$ effector memory T cells, which play an important role in sustaining the anti-tumor effect and preventing tumor recurrence and metastasis. As shown in Figure 5K and L, NP-TCL@APS and NP-TCL increased the number of $CD8^+$ and $CD4^+$ effector memory T cells, with the former exerting a stronger effect. These results indicated that NP-TCL@APS could effectively induce immune responses against tumors.

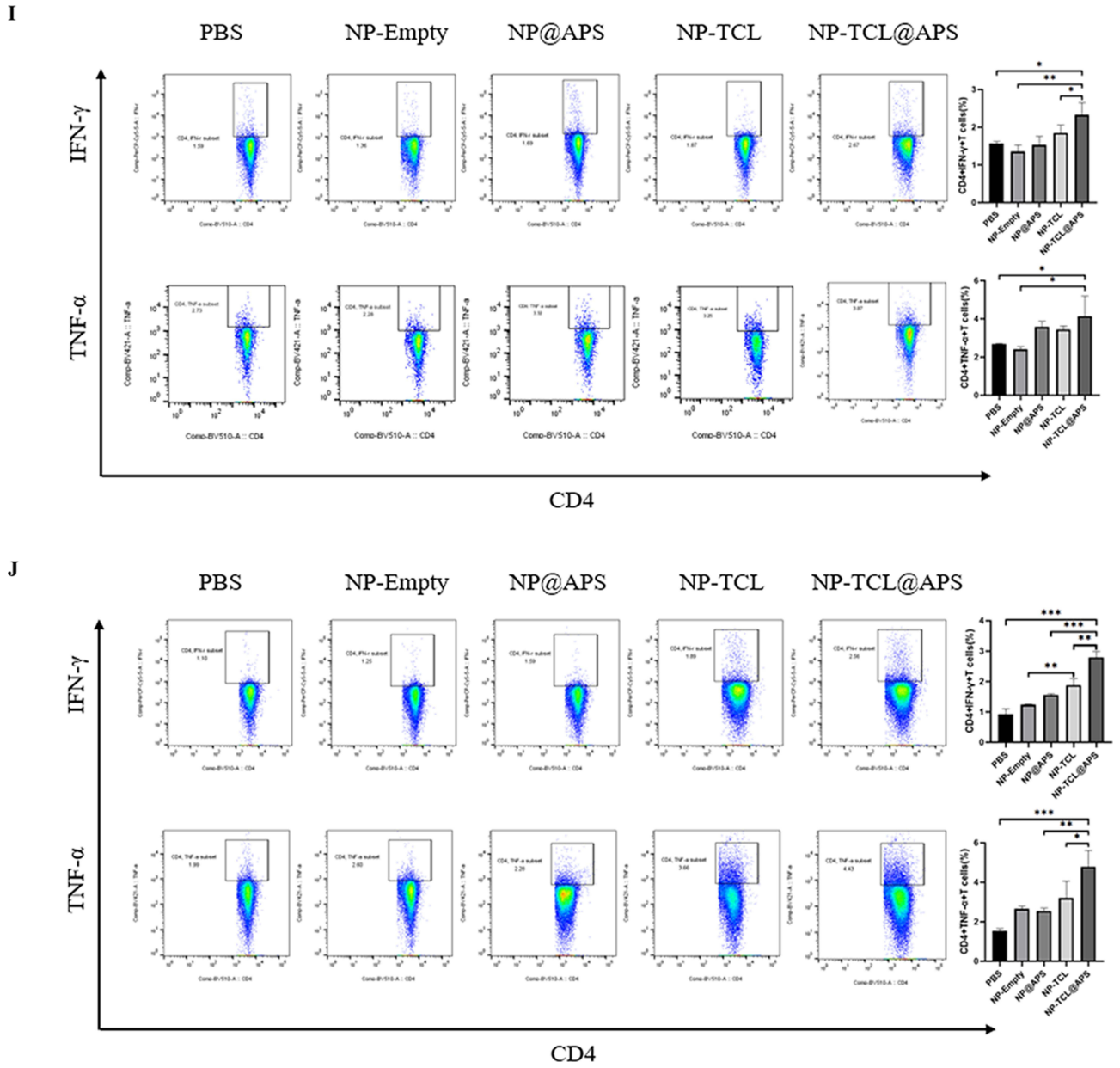

Figure 5 Continued.

Remodeling of the Tumor Microenvironment by NP-TCL@APS

We analyzed the proportions of various immune cells in the tumor microenvironment to explore the mechanism by which NP-TCL@APS enhanced the anti-tumor effect. In the anti-tumor immune response, T cells play a major killing role. Therefore, we investigated whether NP-TCL@APS could mobilize T cells into tumor tissues; the numbers of CD4 and CD8 tumor-infiltrating lymphocytes were measured by flow cytometry. As shown in Figure 6A and B, an increase in both populations of cells was observed in tumors treated with NP-TCL@APS. Furthermore, an increase in M1 macrophages was also observed in the tumor site treated with NP-TCL@APS (Figure 6C).

Regulation of Immunosuppressive Molecules by NP-TCL@APS

T-cell therapy is susceptible to strong immune suppression in the tumor microenvironment., The expression of PD-1 and TIGIT on $CD8^+$ and $CD4^+$ T cells in the tumor, spleen and lymph nodes were measured by flow cytometry to determine whether NP-

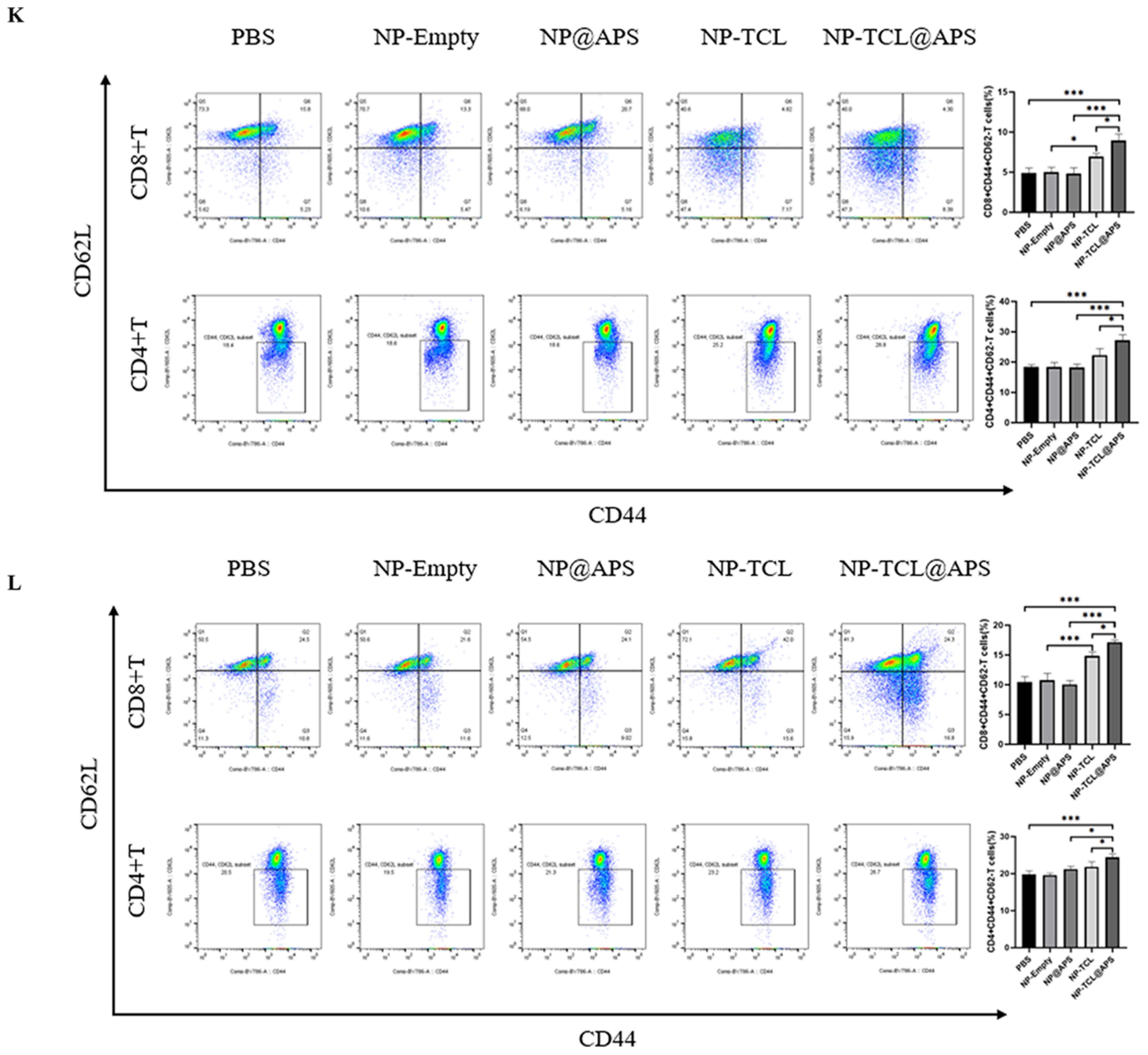

Figure 5 NP-TCL@APS plays an anti-tumor role by activating the immune system. (**A**) DC maturation in the lymph nodes was detected by FCM. (**B**) DC maturation in the spleen was detected by FCM. (**C**) The number of $CD8^+$ T cells in the lymph nodes and spleen was detected by FCM. (**D**) The expression of IFN-γ, GZMB, and TNF-α in $CD8^+$ T cells in the lymph nodes was detected by FCM. (**E**) The expression of IFN-γ, GZMB, and TNF-α in $CD8^+$ T cells in the spleen was detected by FCM. (**F**) The number of $CD4^+$ T cells in the lymph nodes and spleen was detected by FCM. (**G**) The number of Th17 and Treg cells in the lymph nodes was detected by FCM. (**H**) The number of Th17 and Treg cells in the spleen was detected by FCM. (**I**) The expression of IFN-γ and TNF-α in $CD4^+$ T cells in the lymph nodes was detected by FCM. (**J**) The expression of IFN-γ and TNF-α in $CD4^+$ T cells in the spleen was detected by FCM. (**K**) The number of effector memory T cells in the lymph nodes was detected by FCM. (**L**) The number of effector memory T cells in the spleen was detected by FCM. *p <0.05, **p <0.01, ***p <0.001.

TCL@APS can relieve the immune suppression. NP-TCL@APS downregulated the expression of PD-1 and TIGIT in both $CD8^+$ and $CD4^+$ T cells compared with PBS, NP-TCL, and NP@APS (Figure 7A and B). We obtained consistent results in the spleen and lymph nodes (Figure 7C–F).

Discussion

Whereas clinical oncology has relied on targeting oncogenic pathways for decades, lessons learned in recent years by studying immunotherapy mediated durable clinical responses have indicated that mobilization of the host's immune system represents a powerful therapeutic modality.[8] Immunotherapy has demonstrated remarkable therapeutic effects against tumors compared with traditional treatment methods, such as surgery, radiotherapy, and chemotherapy. It plays an

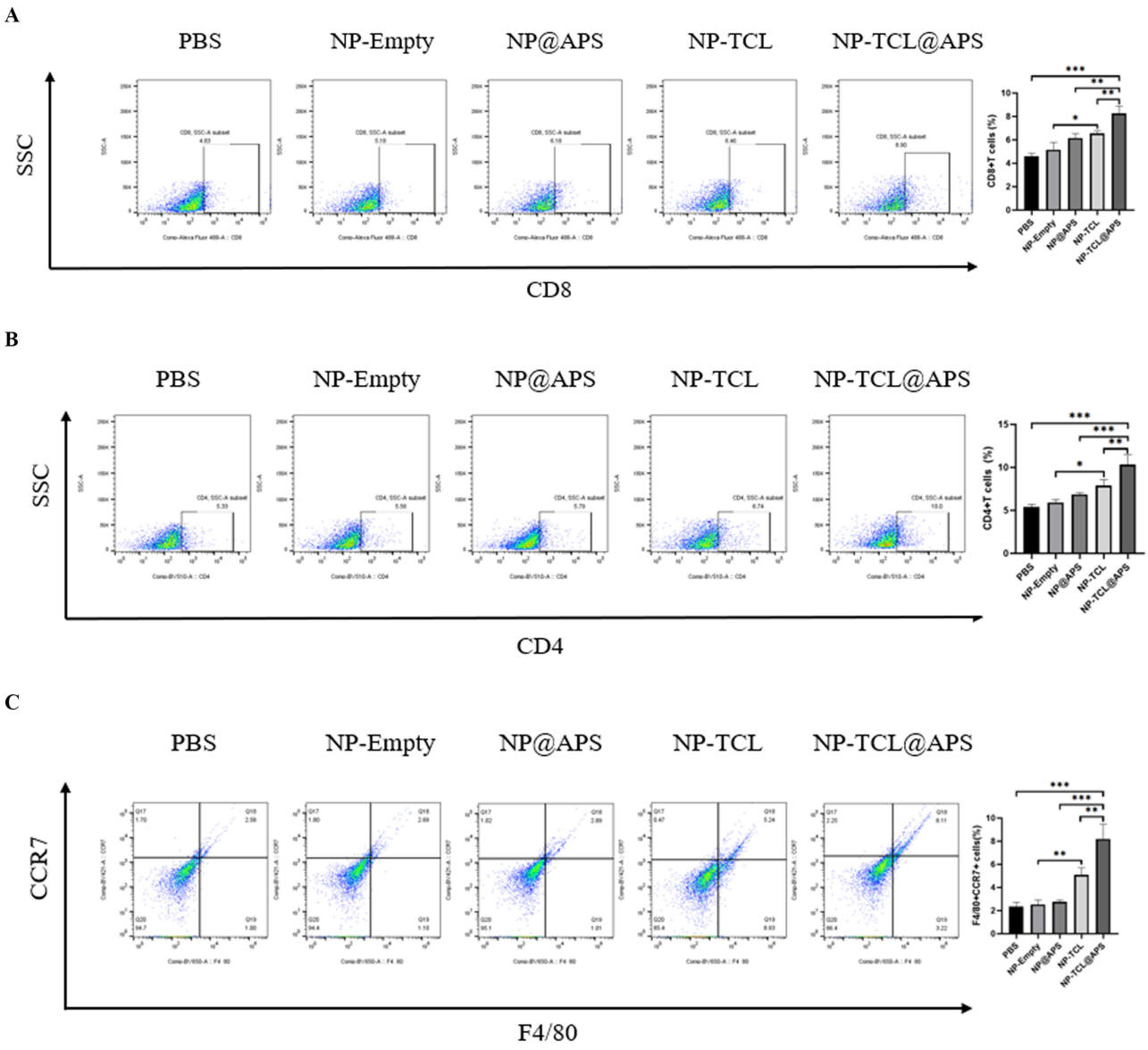

Figure 6 NP-TCL@APS improved the abundance of tumor-infiltrating immune cells to play an anti-tumor role. (**A**) The number of $CD8^+$ T cells in the tumor was detected by FCM. (**B**) The number of $CD4^+$ T cells in the tumor was detected by FCM. (**C**) The number of macrophages in the tumor was detected by FCM. **p* <0.05, ***p* <0.01, ****p* <0.001.

anti-tumor role by mainly activating the immune system of the patient, with high efficacy and a good safety profile.[9] Although immune checkpoint inhibitors (PD-1/PD-L1, cytotoxic T-lymphocyte associated protein 4 [CTLA-4]) have achieved great clinical success, the development of new immunotherapies remains an urgent medical need. Tumor vaccines are considered an effective immunotherapy strategy. This approach aims to overcome immunosuppression in tumors and induce cellular and humoral immune responses that can exert anti-tumor effects.

As APC, DC play a key role in initiating anti-tumor immunity. Stimulation by an antigen triggers adaptive immunity against pathogens or tumors.[10] The most promising strategy involves the delivery of antigens in vivo to DC in the form of nanoparticles, offering numerous advantages over traditional vaccines.[11] The biocompatible PLGA approved by the US Food and Drug Administration has been extensively evaluated as a drug carrier. PLGA nanoparticles overcome major challenges in drug delivery systems, such as the protection of encapsulated drugs from rapid degradation and removal. In addition, co-encapsulation and delivery of antigens and adjuvants to APC can lead to effective DC activation.[12]

Cancer vaccines typically involve exogenous administration of selected tumor antigens combined with adjuvants that activate DCs. The aim of therapeutic cancer vaccines is to stimulate the patient's adaptive immune

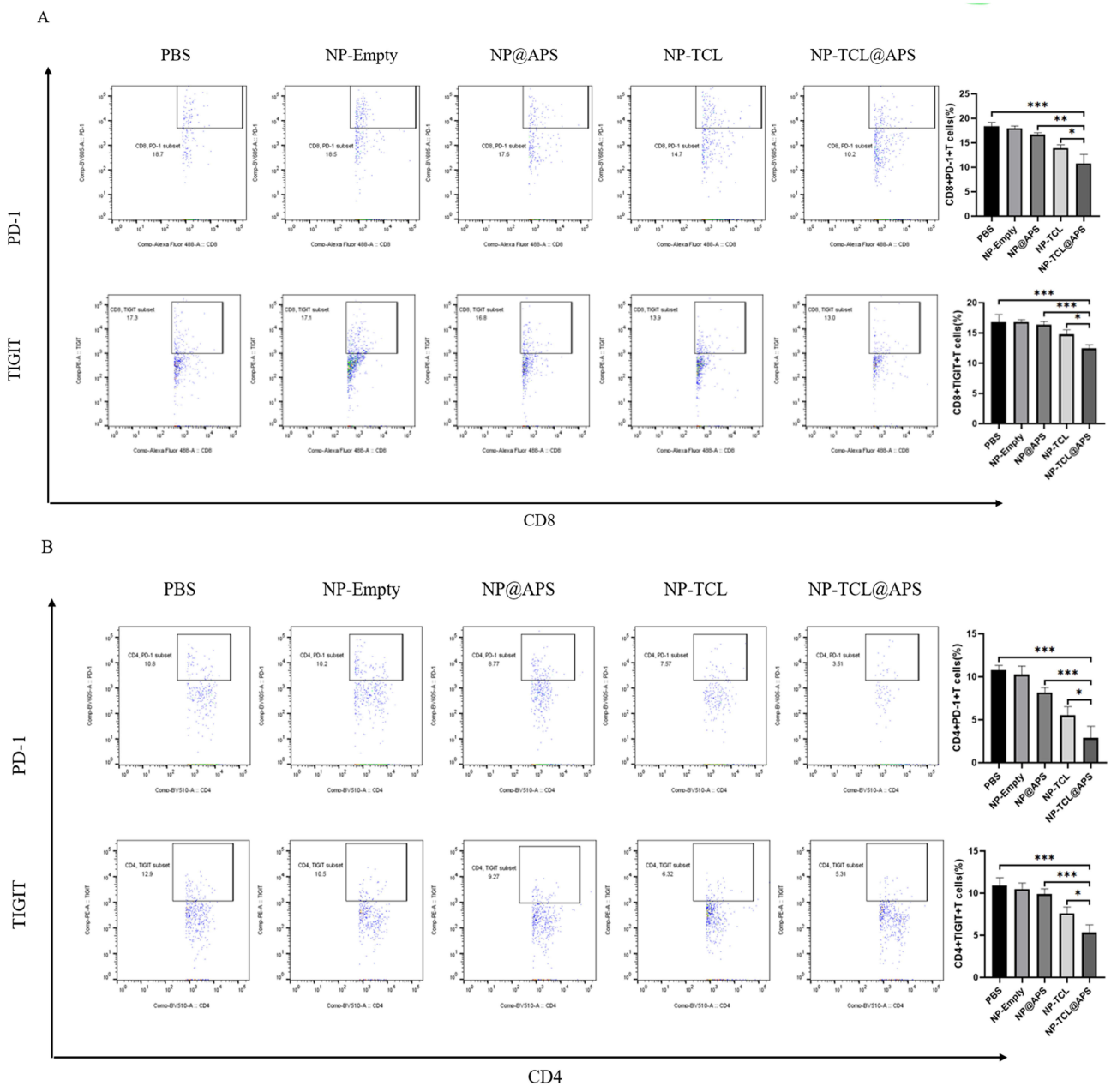

Figure 7 Continued.

system against specific tumor antigens to regain control over tumor growth, induce regression of established tumors.[13] In this study, a spherical NP-TCL@APS with particle size of approximately 250 nm was prepared. The nanovaccine was within the optimal phagocytosis range of DC. Although free TCL could be engulfed by DC, it did not upregulate the expression of MHCII and co-stimulatory molecules CD80 and CD86 on the surface of DC. This may be due to the low dose of free TCL in DC, which is insufficient to cause DC activation. This indicates that PLGA nanoparticles can avoid rapid removal and loss of TCL, as well as improve the delivery of TCL to DC. Cross-presentation of antigens is critical for the generation of CTL-targeting viruses, transplanted cells, and tumor cells. Increasing tumor antigen availability and T cell priming are crucial parameters for the efficient response to anti-cancer vaccines.[14] In our study, the use of PLGA to encapsulate tumor antigens and the sustained release ability of PLGA precisely improved the utilization rate of antigens.

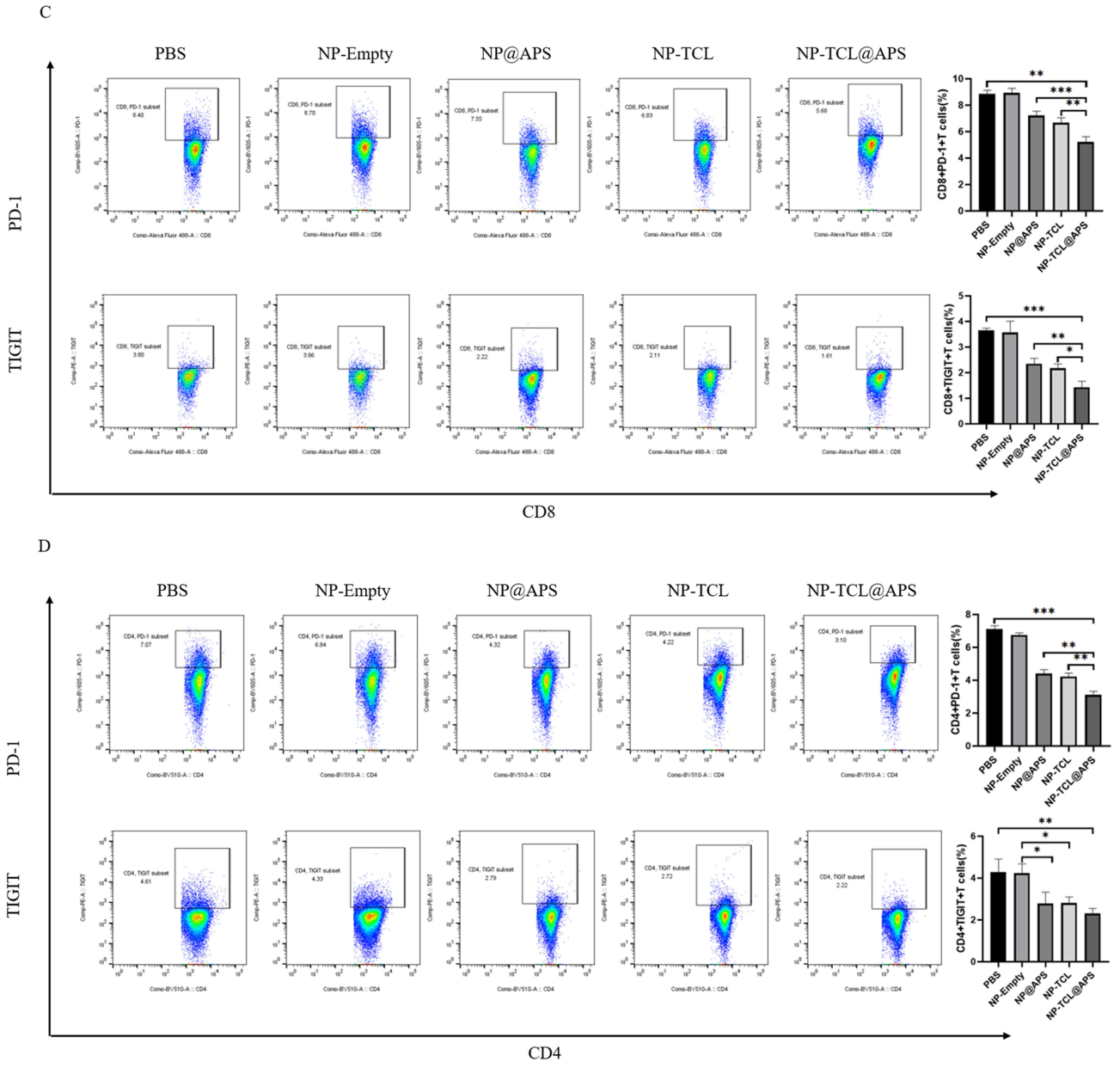

Figure 7 Continued.

In general, immunotherapy has opened a new chapter in cancer treatment and greatly improved the prognosis of CRC, but the therapeutic effect varies greatly among different subtypes of CRC.[15] Furthermore, DC-mediated tumor immunotherapy is highly dependent on the type of antigen.[16] In this study, whole TCL demonstrated its value by containing a wide range of antigenic epitopes from a specific cancer cell and inducing strong polyclonal $CD4^+$ and $CD8^+$ T cell responses through cross-presentation of DC, which may prevent immune escape by tumors.[17] The results of this study showed that, compared with APS nanoparticles, NP-TCL@APS coated with TCL and APS can upregulate the expression of MHCI, MHCII, and CD80 on the surface of spleen DC, as well as that of MHCI and MHCII on the surface of lymph node DC. NP-TCL@APS activates DC through simultaneous delivery of MHCI and MHCII class-restricted antigen epitopes, which in turn induces strong $CD8^+$ and $CD4^+$ T cell responses in tumors, spleen, and lymph nodes. NP-TCL@APS could increase the number of $CD8^+$ T cells and promote the secretion of GZMB, TNF-α, and IFN-γ. Moreover, NP-TCL@APS increased the number of $CD4^+$ T cells and their subsets Th1 and Th17, and promoted the secretion of

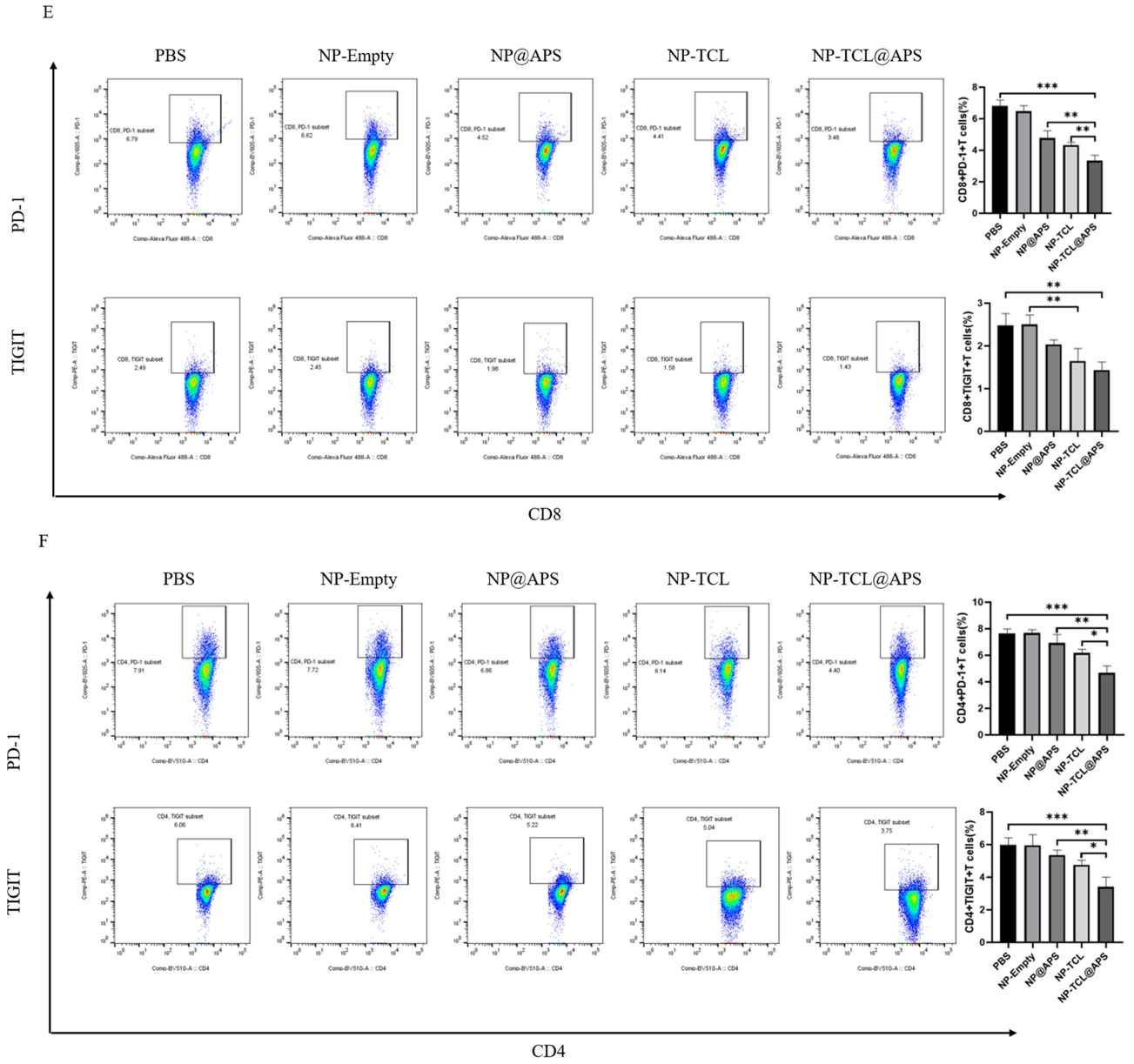

Figure 7 NP-TCL@APS played an anti-tumor role by downregulating the expression of negative immunoregulatory molecules PD-1 and TIGIT. Expression of PD-1 and TIGIT in tumor $CD8^+$ (**A**) and $CD4^+$ (**B**) T cells, detected by FCM. Expression of PD-1 and TIGIT in spleen $CD8^+$ (**C**) and $CD4^+$ (**D**) T cells, detected by FCM. Expression of PD-1 and TIGIT in lymph node $CD8^+$ (**E**) and $CD4^+$ (**F**) T cells, detected by FCM. *p <0.05, **p <0.01, ***p <0.001.

TNF-α by $CD4^+$ T cells. Our results revealed that the whole TCL played a positive role in inducing a broad immune response.

Studies have shown that APS can directly inhibit the proliferation, promote the apoptosis, and regulate the growth cycle of tumor cells, thus delaying disease progression.[18] Our previous studies have shown that APS can inhibit the migration and invasion of CRC cells HT29, SW620, and HCT116; APS can also inhibit the proliferation and promote the apoptosis of HT29 cells. In addition, it has been shown that APS regulate immunoactivity factors, such as IL-2, IL-6, TNF-α, IFN-γ, immunoglobulin A (IgA), IgG, and IgM, secreted by immune cells (eg, macrophages, natural killer cells, DC, T lymphocytes, B lymphocytes, and microglia).[19,20] In this study, APS improved the efficiency of TCL uptake by DC in vitro, promoted DC maturation by upregulating the expression of MHCII and CD80, and induced lymphocyte proliferation and $CD8^+$ T cell activation. These effects contributed to the killing of tumor cells. In vivo studies revealed that, compared with NP-Empty, NP@APS could

significantly inhibit tumor growth and induce significant immune response, which reshapes the immune microenvironment. In future research, we will continue to delve into the anti-tumor function and specific mechanisms of APS.

Collectively, these positive data clearly demonstrate the great potential of NP-TCL@APS as vaccine therapy in suppressing tumor growth. Besides, we confirmed that NP-TCL@APS can stimulate $CD8^+$ and $CD4^+$ effector memory T cells, which proves that the vaccine has immune killing and long-term memory effects. Nevertheless, additional research involving a recurrence or metastasis model is necessary to verify the effects of this approach.

Conclusion

In this study, we successfully prepared a nanovaccine termed NP-TCL@APS, which can promote the maturation of DC and induce strong responses by T lymphocytes to exert anti-tumor effects. Moreover, this method provides new ideas and strategies for the immunotherapy of cancer. Firstly, PLGA was shown to be a safe and non-toxic vaccine delivery vehicle. Secondly, PLGA possesses a sustained-release function. As an 'antigen library', TCL played a crucial role in the activation process of DC to further induce extensive and strong responses by $CD8^+$ and $CD4^+$ T cells. As a vaccine adjuvant, APS significantly promoted the maturation of DC and the uptake and cross-presentation of TCL by DC, which could stimulate an anti-tumor immune response. Furthermore, this strategy is highly extensible and provides a valuable reference for the preparation of anti-tumor vaccines.

Abbreviations

CRC, Colorectal Cancer; DC, Dendritic cells; PLGA, Poly(lactic-co-glycolic acid); APS, Astragalus polysaccharides; TCL, Tumor cell lysate; APC, Antigen presenting cell; CTL, Cytotoxic T lymphocytes; TAA, Tumor associated antigen; PDI, Polymer dispersity index; CFSE, carboxyfluorescein succinimidyl ester; FCM, flow cytometry; NP, nanoparticle; TIGIT, T cell immunoreceptor with Ig and ITIM domains; GZMB, granzyme B; IFN-γ, interferon-γ; Th17, T helper cell 17; TNF-α, tumor necrosis factor-α; Treg, regulatory T cell.

Data Sharing Statement

The datasets used and/or analyzed during the current study are available from the corresponding author upon reasonable request.

Ethics Approval and Consent to Participate

All animal experiments were approved by the Experimental Animal Ethics Committee of Ningxia Medical University (Yinchuan, China).

Funding

This research was supported by the National Natural Science Foundation of China (NO: 81760437,82160548,82260819), Natural Science Foundation of Ningxia Province (NO:2020AAC03183,2021AAC02011,2023AAC02042,2023AAC02082) and Key Research and Development Program of Ningxia Province (NO: 2023BEG02013).

Disclosure

The authors declare that there are no conflicts of interest.

References

1. Wei F, Tang L, He Y, et al. BPIFB1 (LPLUNC1) inhibits radioresistance in nasopharyngeal carcinoma by inhibiting VTN expression. *Cell Death Dis*. 2018;9(4):432. doi:10.1038/s41419-018-0409-0
2. Joshi VB, Geary SM, Gross BP, Wongrakpanich A, Norian LA, Salem AK. Tumor lysate-loaded biodegradable microparticles as cancer vaccines. *Expert Rev Vaccines*. 2014;13(1):9–15. doi:10.1586/14760584.2014.851606
3. Su Y, Zhang B, Sun R, et al. PLGA-based biodegradable microspheres in drug delivery: recent advances in research and application. *Drug Deliv*. 2021;28(1):1397–1418. doi:10.1080/10717544.2021.1938756
4. Rocha CV, Goncalves V, Da SM, Banobre-Lopez M, Gallo J. PLGA-based composites for various biomedical applications. *Int J Mol Sci*. 2022;23(4). doi:10.3390/ijms23042034

5. Peres C, Matos AI, Conniot J, et al. Poly(lactic acid)-based particulate systems are promising tools for immune modulation. *Acta Biomater*. 2017;48:41–57. doi:10.1016/j.actbio.2016.11.012
6. Patel MK, Tanna B, Gupta H, Mishra A, Jha B. Physicochemical, scavenging and anti-proliferative analyses of polysaccharides extracted from psyllium (plantago ovata forssk) husk and seeds. *Int J Biol Macromol*. 2019;133:190–201. doi:10.1016/j.ijbiomac.2019.04.062
7. Pang C, Yuan B, Ren K, et al. Activates B lymphocytes and enhanced immune response: a promising adjuvant based on PLGA nanoparticle to improve the sensitivity of ZEN monoclonal antibody. *Talanta*. 2024;274:126005. doi:10.1016/j.talanta.2024.126005
8. Sahin U, Tureci O. Personalized vaccines for cancer immunotherapy. *Science*. 2018;359(6382):1355–1360. doi:10.1126/science.aar7112
9. Zhang J, Tavakoli H, Ma L, Li X, Han L, Li X. Immunotherapy discovery on tumor organoid-on-a-chip platforms that recapitulate the tumor microenvironment. *Adv Drug Deliv Rev*. 2022;187:114365. doi:10.1016/j.addr.2022.114365
10. Huang L, Rong Y, Tang X, et al. Engineered exosomes as an in situ DC-primed vaccine to boost antitumor immunity in breast cancer. *Mol Cancer*. 2022;21(1):45. doi:10.1186/s12943-022-01515-x
11. Wang W, Liu Z, Zhou X, et al. Ferritin nanoparticle-based SpyTag/SpyCatcher-enabled click vaccine for tumor immunotherapy. *Nanomedicine*. 2019;16:69–78. doi:10.1016/j.nano.2018.11.009
12. Danhier F, Ansorena E, Silva JM, Coco R, Le breton A, Preat V. PLGA-based nanoparticles: An overview of biomedical applications. *J Control Release*. 2012;161(2):505–522. doi:10.1016/j.jconrel.2012.01.043
13. Saxena M, van der Burg SH, Melief C, Bhardwaj N. Therapeutic cancer vaccines. *Nat Rev Cancer*. 2021;21(6):360–378. doi:10.1038/s41568-021-00346-0
14. Accolla RS, Buonaguro L, Melief C, Rammensee HG, Bassani-Sternberg M. Editorial: novel strategies for anti-tumor vaccines. *Front Immunol*. 2019;10:3117. doi:10.3389/fimmu.2019.03117
15. Zheng X, Ma Y, Bai Y, et al. Identification and validation of immunotherapy for four novel clusters of colorectal cancer based on the tumor microenvironment. *Front Immunol*. 2022;13:984480. doi:10.3389/fimmu.2022.984480
16. Sadeghi NS, Bolhassani A, Aghasadeghi MR. Tumor cell-based vaccine: An effective strategy for eradication of cancer cells. *Immunotherapy*. 2022;14(8):639–654. doi:10.2217/imt-2022-0036
17. Liau LM, Ashkan K, Brem S, et al. Association of autologous tumor lysate-loaded dendritic cell vaccination with extension of survival among patients with newly diagnosed and recurrent glioblastoma: A Phase 3 prospective externally controlled cohort trial. *JAMA Oncol*. 2023;9(1):112–121. doi:10.1001/jamaoncol.2022.5370
18. Tao X, Zhang X, Feng F. Astragalus polysaccharide suppresses cell proliferation and invasion by up-regulation of miR-195-5p in non-small cell lung cancer. *Biol Pharm Bull*. 2022;45(5):553–560. doi:10.1248/bpb.b21-00634
19. Wan X, Yin Y, Zhou C, et al. Polysaccharides derived from Chinese medicinal herbs: A promising choice of vaccine adjuvants. *Carbohydr Polym*. 2022;276:118739. doi:10.1016/j.carbpol.2021.118739
20. Abuelsaad AS. Supplementation with Astragalus polysaccharides alters Aeromonas-induced tissue-specific cellular immune response. *Microb Pathog*. 2014;66:48–56. doi:10.1016/j.micpath.2013.12.005